

# Investigation of Cu-poor and Cu-rich Cu(In,Ga)Se<sub>2</sub>/CdS interfaces using hard X-ray photoelectron spectroscopy

B. Ümsür<sup>a</sup>, W. Calvet<sup>a</sup>, B. Höpfner<sup>a</sup>, A. Steigert<sup>a</sup>, I. Lauer<sup>a</sup>, M. Gorgoi<sup>a</sup>, K. Prietzel<sup>a</sup>, H.A. Navirian<sup>a</sup>, C.A. Kaufmann<sup>a</sup>, T. Unold<sup>a</sup>, M. Ch. Lux-Steiner<sup>a,b</sup>

<sup>a</sup> Helmholtz-Zentrum-Berlin, Hahn-Meitner-Platz 1, D-14109 Berlin, Germany

<sup>b</sup> Freie Universität Berlin, Department of Physics, Arnimallee 14, D-14195 Berlin, Germany

## Keywords:

Chalcopyrite  
Hard X-ray photoelectron spectroscopy  
Cd diffusion  
Interface

## Abstract

Cu-poor and Cu-rich Cu(In,Ga)Se<sub>2</sub> (CIGSe) absorbers were used as substrates for the chemical bath deposition of ultrathin CdS buffer layers in the thickness range of a few nanometers in order to make the CIGSe/CdS interface accessible by hard X-ray photo-emission spectroscopy. The composition of both, the absorber and the buffer layer as well as the energetics of the interface was investigated at room temperature and after heating the samples to elevated temperatures (200 °C, 300 °C and 400 °C). It was found that the amount of Cd after the heating treatment depends on the near surface composition of the CIGSe absorber. No Cd was detected on the Cu-poor surface after the 400 °C treatment due to its diffusion into the CIGSe layer. In contrast, Cd was still present on the Cu-rich surface after the same treatment at 400 °C.

## 1. Introduction

Thin film solar cells based on polycrystalline Cu(In,Ga)Se<sub>2</sub> (CIGSe) absorbers already reach maximum conversion efficiencies above 20% on the laboratory scale [1]. Besides the defects in the absorber material, the interface between the CIGSe absorber and the CdS buffer layer plays an important role with respect to band alignment and appearance of interface states limiting the solar power conversion efficiency [2]. It is assumed that intrinsic surface properties of the CIGSe absorber such as composition, crystal structure, texture and termination are crucial regarding the formation of the CIGSe/CdS/ZnO heterocontact [3]. In the present work, differently grown CIGSe absorbers with surface concentrations of  $[Cu]/([In] + [Ga]) = 0.79$  (Cu-poor) and 1.03 (Cu-rich) were used for the experiment described in this publication. These compositions were chosen because the Cu-poor composition is close to the optimum composition for high-efficiency devices in our lab [4] and therefore represents the “standard absorber”, while the Cu-rich composition, although close to the theoretical stoichiometry, behaves fundamentally differently from even slightly Cu-poor absorbers [5].

Ultrathin CdS layers were deposited by chemical bath deposition (CBD) on both absorbers under the same conditions with an estimated thickness of less than 10 nm which allows the simultaneous investigation of the CIGSe absorber and the CdS buffer layer as well as the corresponding interface region using hard X-ray photo-emission spectroscopy (HAXPES) with excitation energies of 3000 eV and 6000 eV. The aim was to analyze the interface formation especially focusing on Cu and Cd species which are believed to play an important role in this process. Additionally, possible diffusion phenomena were investigated in situ under ultrahigh vacuum

(UHV) conditions after annealing at temperatures of 200 °C, 300 °C and 400 °C.

## 2. Experimental details

### 2.1. Sample preparation

Polycrystalline CIGSe thin films have been grown on molybdenum coated soda lime glass (SLG) substrates using a modified three stage coevaporation process. Details on this process are given in reference [6]. The Cu-content of the completed CIGSe film is mainly determined by the duration of the third stage where the shutters of the In-, Ga-, and Se-sources are opened while the shutter of the Cu-source is closed until the stoichiometric point of the compound material is reached as measured with optical real-time methods. Continuing the evaporation of In–Ga–Se results in the deposition of a Cu-poor CIGSe absorber. By shortening the third stage accordingly, Cu-rich absorbers can be produced. For the experiment at hand, one Cu-poor and one Cu-rich absorber were grown on 5 cm × 5 cm large SLG substrates. Altogether, two Cu-rich and two Cu-poor samples with a size of 4 mm × 8 mm were cut out so that two of them could be mounted on one sample holder at once for the subsequent HAXPES measurements. In order to remove segregated Cu<sub>x</sub>Se or surface oxide phases, all samples were etched in an NaCN containing aqueous solution (5%) for 3 min at room temperature (RT). Afterwards, they were rinsed with deionized water and dried in an ultrapure gaseous nitrogen stream. While one set of the samples (Cu-rich and Cu-poor) was transferred to the UHV based analysis chamber for HAXPES measurements using a special transport box which was flooded with nitrogen, the other samples

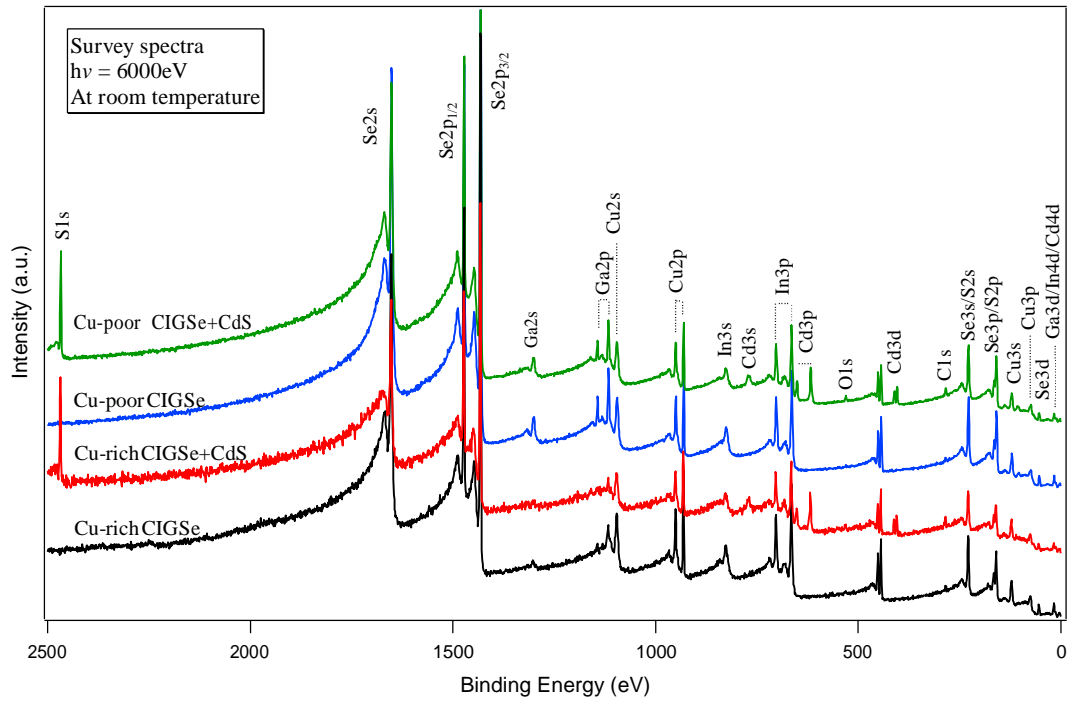


**Fig. 1.** XP survey spectra of bare CIGSe and CBD-CdS/CIGSe samples at 6000 eV excitation energy measured at room temperature.

were treated further. Thin CdS layer was deposited on top of them by CBD using 0.0189 M cadmium acetate dihydrate ( $\text{Cd}(\text{C}_2\text{H}_3\text{O}_2)_2 \cdot 2\text{H}_2\text{O}$ ) in 11.25 ml aqueous  $\text{NH}_3$  (25%) and 0.9565 M thiourea ( $\text{H}_2\text{NCSNH}_2$ ) in 100 ml water which were mixed together and filled up by distilled water to a total volume of 150 ml. The samples were simultaneously dipped into the chemical bath for 45 s at 60 °C leading to ultrathin CdS layers in the thickness range of 10 nm as estimated from the standard CdS deposition process. These samples were also transferred to the high kinetic energy (HIKE) analysis chamber using the same transport box.

## 2.2. Sample characterization

The HAXPES experiments were performed at the HIKE endstation operated at the KMC-1 beamline located at the BESSY II synchrotron facility in Berlin, providing variable photon energies up to 12 keV. For the experiment which is presented in this paper, excitation energies of 3000 eV and 6000 eV with variable information depth were used, roughly calculated as 20 nm for 6000 eV and 10 nm for 3000 eV respectively. The analysis system at the HIKE endstation consists of a R4000 hemispherical photoelectron spectrometer manufactured by Scienta GammaData which is optimized for high kinetic energy. All spectra in this work were recorded at a constant pass energy of 200 eV. The X-ray beam was horizontally polarized and hits the sample in grazing incidence under an angle of 3° towards the surface. The photoelectrons were detected in the polarization plane perpendicular to the beam while its intensity was monitored using an  $\text{N}_2$  ionization chamber and

kept constant for all measurements (top-up mode of the storage ring). The spot size of the beam under the grazing incidence conditions was in the range of 2 mm in diameter, which reduces the influence of the surface roughness and inhomogeneity of Cd thickness on the accuracy of the measurements. The entrance slit of the electron analyzer was fixed to 0.5 mm. In addition, the samples were imaged with a Zeiss Leo 1530 scanning electron microscope (SEM).

## 3. Results

In Fig. 1 the survey spectra of bare CIGSe samples and the CdS covered CIGSe samples recorded at room temperature are shown for 6000 eV excitation energy in the binding energy range from 0 to 2500 eV.

Since the thickness of the CdS film was limited to few nanometers, photoemission signals originating from the CIGSe absorber are present in all spectra due to the increased kinetic energy of the considered electrons, implying an increased information depth. In addition, cadmium and sulfur related peaks appear in the spectra for the CdS covered samples, as expected. Moreover, small quantities of carbon and oxygen are only detectable on the wet-chemically treated CIGSe/CdS samples due to the usage of aqueous solutions for the deposition of CdS — an indication that carbon and oxygen containing species are incorporated into the CdS film during growth. This aspect is not considered in the following, thus neglected.

Fig. 2 shows top view images of the samples obtained with SEM of the bare Cu-poor (a) and Cu-rich (b) CIGSe samples as well as the CdS coated

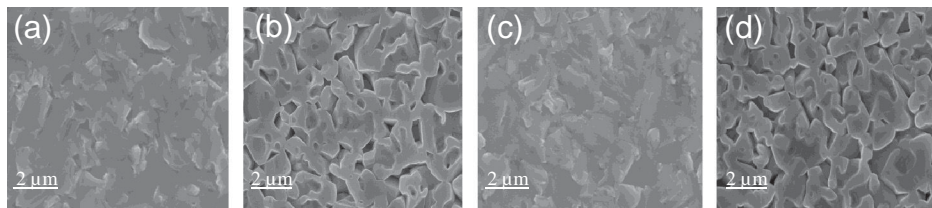


**Fig. 2.** SEM top view images of Cu-poor CIGSe (a) and CIGSe/CdS (c) and Cu-rich CIGSe (b) and CIGSe/CdS (d) samples which were measured with XPS (see Fig. 1). The images were taken after the last annealing step in UHV at 400 °C.

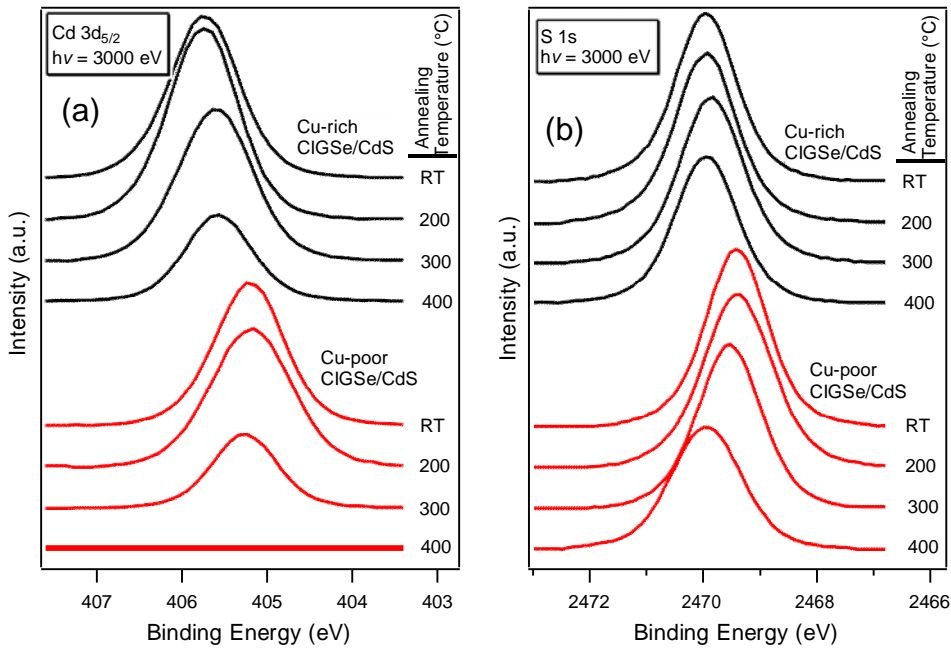


**Fig. 3.** XP spectra of the (a) Cd 3d<sub>5/2</sub> and (b) S 1s photoemission signals of the CIGSe/CdS samples recorded at the HIKE end station at BESSY II using 3000 eV excitation energy. The measurements were performed at room temperature (RT) and after a series (at 200 °C, 300 °C, and 400 °C) of in-situ annealing steps in UHV.

Cu-poor (c) and Cu-rich (d) CIGSe samples after the final annealing step in UHV. It can be seen that the samples are polycrystalline.

In contrast to the Cu-poor samples, the Cu-rich samples show an increased roughness which is attributed to the NaCN based etching process which is known to remove superficial Cu<sub>x</sub>Se phases. The morphology of these samples is dominated by cavities surrounded by linked structures which seem to be equally truncated on the same height. On closer inspection, the size of the grains appears to be very large with dimensions of up to several micrometers and with grain boundaries forming deep valleys. The Cu-poor samples are less affected by the NaCN etching process leaving surfaces which are smoother but somehow stronger declined on the microscopic scale. The truncation of the topmost layer as observed on the Cu-rich samples is not visible on Cu-poor samples. In both cases, step-like formations with several nanometer dilatations are observed, pointing to a [112] orientated faceting of Cu-poor areas of the grains [5]. With energy dispersive X-ray spectroscopy (EDX) attached to the SEM system, no Cd could be detected on the CdS coated CIGSe samples

indicating that the amount of Cd is below the detection threshold of the EDX system. For a detailed analysis of the X-ray photoemission (XP) spectra, the Cu 2p<sub>3/2</sub>, In 3p<sub>3/2</sub>, Ga 2p<sub>3/2</sub>, Se 2p<sub>3/2</sub>, Cd 3d<sub>5/2</sub>, and S 1s core level peaks were measured with higher resolution. In Fig. 3 dedicated Cd 3d<sub>5/2</sub> and S 1s spectra are shown for each annealing step using 3000 eV excitation energy. The samples were annealed consecutively at 200 °C, 300 °C and 400 °C (heating with about 20 °C/min) for 10 min. After each annealing step subsequent X-ray photoemission spectroscopy (XPS) measurements were performed at room temperature. For temperatures up to 300 °C, the dependency of the Cd 3d<sub>5/2</sub> peak on the annealing process is similar for both, the Cu-poor (red lines) and Cu-rich (black lines) samples. But for 400 °C, the Cd 3d<sub>5/2</sub> peak of the Cu-poor CIGSe/CdS system completely vanishes whereas for the Cu-rich CIGSe/CdS system it is only damped and still present.

In contrast to the Cd 3d<sub>5/2</sub> signal, the S 1s peak intensities are less affected in both cases; there is still sulfur on the surface in a reasonable amount. Fig. 4 shows the elemental concentrations of the near surface

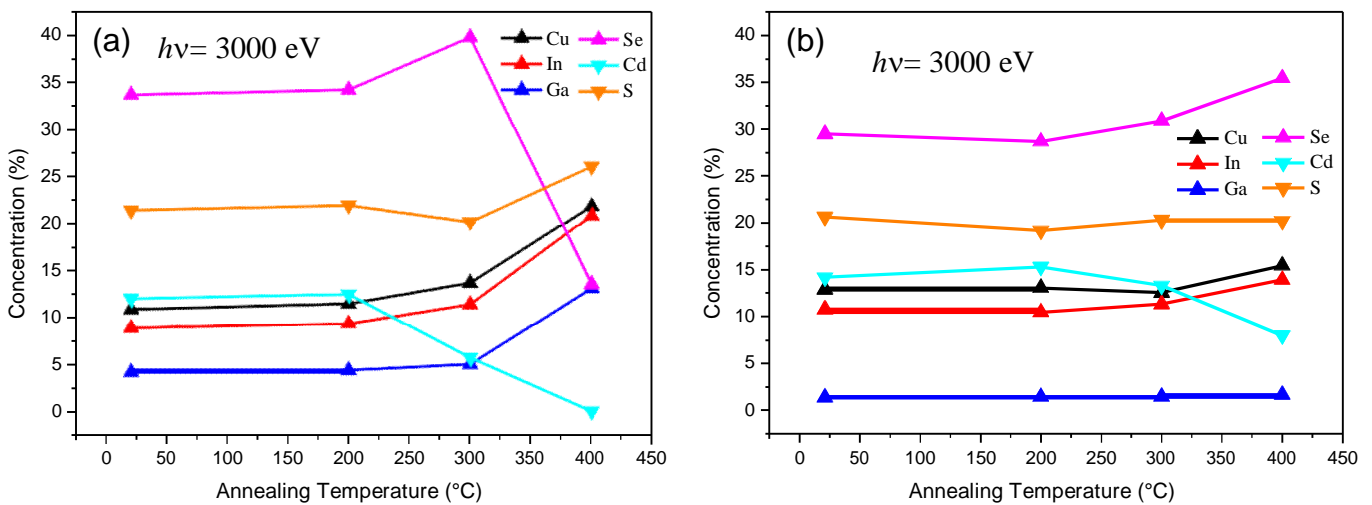


**Fig. 4.** Concentrations of the Cu, In, Ga, Se, Cd, and S species of the CdS coated CIGSe samples: (a) Cu-poor and (b) Cu-rich. The concentration values were calculated from the line intensities of the corresponding core level peaks which were recorded at 3000 eV excitation energy.

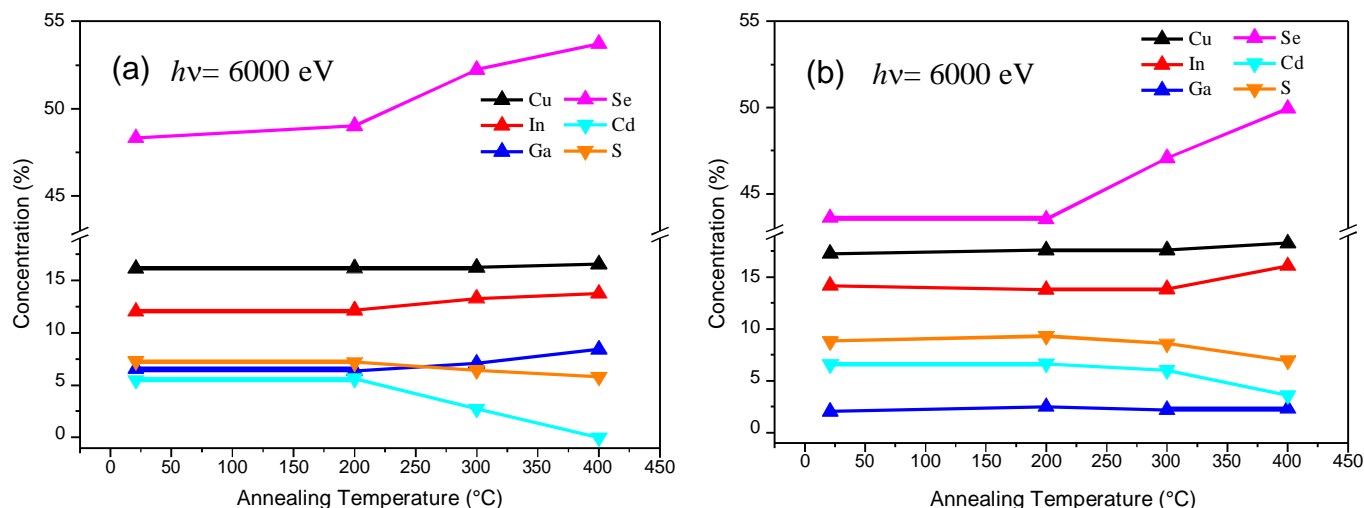


**Fig. 5.** Concentrations of the Cu, In, Ga, Se, Cd, and S species of the CdS coated CIGSe samples: (a) Cu-poor and (b) Cu-rich. The concentration values were calculated from the line intensities of the corresponding core level peaks which were recorded at 6000 eV excitation energy.

elements Cu, In, Ga, Se, Cd, and S for all applied annealing steps. They were calculated from the corresponding photoemission core level peaks obtained for 3000 eV excitation energy, assuming a homogenous element distribution at the surface. Before starting the evaluation, all spectra were corrected with respect to their binding energy using the position of the Au  $4f_{7/2}$  peak at 84.0 eV [7]. After subtraction of a Shirley background the spectra were integrated to determine the respective line intensities. They were then normalized to the corresponding inelastic mean free path  $\lambda$  (calculated by the TPP-2M formula [8] using the QUASES code [9]), the transmission function of the analyzer  $T$ , and the partial subshell photoionization cross-sections  $d\sigma/d\Omega$  which is tabulated [10,11] to make them comparable.

In contrast to Fig. 4, the elemental concentrations of the same elements are shown in Fig. 5 as obtained from photoemission core level peaks recorded at 6000 eV excitation energy. The information depth is now increased by a factor of 2 from 10 nm to 20 nm.

#### 4. Discussion

The most striking result is the complete disappearance of the cadmium signal from the CdS-coated, Cu-poor surface after annealing at 400 °C, which is in strong contrast to the observation of the remaining Cd on the Cu-rich surface. Since both samples were heated simultaneously on the same sample holder and both samples had been coated in the same CBD process, giving rise to the same thickness of CdS on the surface, evaporation of CdS can be ruled out to explain the disappearance of the Cd signal. This is also supported by the presence of sulfur on both samples even after the 400 °C treatment, because CdS

evaporates congruently, i.e. similar amounts of Cd and S should evaporate. Therefore we believe that the disappearance of Cd is due to the diffusion of Cd into the highly defective, Cu-poor surface of the Cu-poor grown sample where  $Cd^{2+}$  may occupy empty Cu sites. On the Cu-rich sample, the density of Cu vacancies is much smaller, allowing less  $Cd^{2+}$  to penetrate the surface and disappear (for a surface sensitive method) into the near-surface bulk of the absorber. Thus the disappearance of Cd on the Cu-poor surface is interpreted as a dilution of Cd up to a concentration which is not detectable by XPS anymore, while most of the Cd stays on the surface of the Cu-rich sample within the detection limit of XPS. The diffusion of Cd into CIGSe has been the subject of several papers, both theoretical [12,13] and experimental [14,15] and it is assumed that the substitution of  $Cu^+$  by  $Cd^{2+}$  is an important step in the interface formation [2].

The concentrations of Cu, In, Ga, Se and S species within the information depth of about 20 nm vary in a similar manner during the annealing process for both the Cu-poor and Cu-rich CIGSe/CdS samples (Fig. 5). However, in the more surface near region (~10 nm) the concentration of Se on the Cu-poor CIGSe/CdS sample drops dramatically just after annealing at 400 °C (Fig. 4-a). We believe that this is due to a single event that occurred during the measurement, which causes the erroneous data acquisition. Therefore we currently disregard this data point. This drop in the signal intensity is also the reason, why the concentrations of the other species on the surface are increasing at those temperatures since the sum of species related concentrations for the calculation was kept constant.

The relative binding energy shifts of the core level peaks obtained with excitation energies of 3000 eV and 6000 eV are listed in Tables 1 and 2 with

**Table 1**

Relative shifts of the binding energies of the considered peaks with respect to the room temperature measurements as the reference. The measurements were performed at 3000 eV excitation energy and the error is assumed to be  $\pm 0.1$  eV.

$\Delta$ (eV)	Cu-poor								Cu-rich							
	CIGSe				CIGSe/CdS				CIGSe				CIGSe/CdS			
	T (°C)															
	RT	200	300	400	RT	200	300	400	RT	200	300	400	RT	200	300	400
$E_v - E_f$	0.0	–	0.1	0.2	0.0	–0.1	0.0	0.1	0.0	0.0	0.1	0.3	0.0	0.0	–0.1	–0.2
Cu $2p_{3/2}$	0.0	–	0.1	0.3	0.0	0.0	0.1	0.2	0.0	0.1	0.3	0.5	0.0	0.1	0.0	–0.1
In $3p_{3/2}$	0.0	–	0.1	0.3	0.0	0.0	0.0	0.2	0.0	0.1	0.2	0.4	0.0	0.0	–0.1	–0.1
Ga $2p_{3/2}$	0.0	–	0.1	0.3	0.0	0.0	0.0	0.3	0.0	0.1	0.2	0.4	0.0	0.0	0.0	–0.1
Se $2p_{3/2}$	0.0	–	0.1	0.3	0.0	0.0	0.0	0.3	0.0	0.1	0.2	0.4	0.0	0.0	–0.1	–0.1
Cd $3d_{5/2}$	–	–	–	–	0.0	0.0	0.1	–	–	–	–	–	0.0	0.0	–0.1	–0.2
S $1s$	–	–	–	–	0.0	0.0	0.1	0.5	–	–	–	–	0.0	0.0	–0.1	0.0

**Table 2**

Relative shifts of the binding energies of the considered peaks with respect to the room temperature measurements as the reference. The measurements were performed at 6000 eV excitation energy and the error is assumed to be  $\pm 0.1$  eV.

$\Delta$ (eV)	Cu-poor								Cu-rich							
	CIGSe				CIGSe/CdS				CIGSe				CIGSe/CdS			
	T (°C)															
	RT	200	300	400	RT	200	300	400	RT	200	300	400	RT	200	300	400
$E_v-E_f$	0.0	-0.2	0.5	0.4	0.0	-0.1	0.4	0.2	0.0	0.0	-0.3	-0.1	0.0	0.1	-0.1	-0.3
Cu 2p <sub>3/2</sub>	0.0	-0.4	-0.2	0.0	0.0	-0.4	-0.3	-0.3	0.0	0.1	0.2	0.3	0.0	0.1	0.1	-0.1
In 3p <sub>3/2</sub>	0.0	-0.5	-0.2	0.1	0.0	-0.5	-0.3	-0.1	0.0	0.1	0.1	0.3	0.0	0.1	0.2	0.0
Ga 2p <sub>3/2</sub>	0.0	-0.5	-0.1	0.1	0.0	-0.3	-0.2	-0.1	0.0	0.1	0.1	0.2	0.0	0.1	0.2	0.0
Se 2p <sub>3/2</sub>	0.0	-0.5	-0.1	0.1	0.0	-0.2	-0.2	-0.1	0.0	0.1	0.1	0.2	0.0	0.2	0.2	0.0
Cd 3d <sub>5/2</sub>	-	-	-	-	0.0	-0.5	-0.3	-	-	-	-	-	0.0	0.1	0.0	-0.1
S 1s	-	-	-	-	0.0	-0.3	-0.1	0.4	-	-	-	-	0.0	0.1	0.1	0.1

respect to the room temperature measurement. In Table 1 the values for the Cu-poor CIGSe sample at 200 °C are missing because of an experimental failure. However, similar shifts of core level peaks and valence band maximum  $E_v-E_f$  point to an annealing induced band bending at the CIGSe/CdS interface on both, the Cu-poor and Cu-rich samples. A significant shift in the binding energy of the S 1s photoemission signal occurs after the disappearance of Cd 3d<sub>5/2</sub> signal at 400 °C for the Cu-poor CIGSe/CdS sample, which could be assigned to a change in the chemical environment of the sulfur atoms. Nevertheless, the uncertainty in determining the chemical shifts is in the order of the differences between each individual value listed in the tables. Therefore, further experiments are required to investigate the reproducibility of those shifts and to give a complete picture of interface formation during the annealing of CIGSe/CdS system in ultrahigh vacuum.

### Acknowledgments

The authors thank C. Ferber for the SEM images. One of the authors (B. Ümsür) gratefully acknowledges the financial support from the Ministry of Education of the Republic of Turkey.

### References

- [1] A. Chirilă, P. Reinhard, F. Pianezzi, P. Bloesch, A.R. Uhl, C. Fella, et al., Potassium-induced surface modification of Cu(In, Ga)Se<sub>2</sub> thin films for high-efficiency solar cells, *Nat. Mater.* 12 (2013) 1107.
- [2] R. Klenk, Characterisation and modelling of chalcopyrite solar cells, *Thin Solid Films* 387 (2001) 135.

- [3] J.A.M. AbuShama, S. Johnston, T. Moriarty, G. Teeter, K. Ramanathan, R. Noufi, Properties of ZnO/CdS/CuInSe<sub>2</sub> solar cells with improved performance, *Prog. Photovoltaics Res. Appl.* 12 (2004) 39.
- [4] C.A. Kaufmann, T. Unold, D. Abou-Ras, J. Bundesmann, A. Neisser, R. Klenk, et al., Investigation of coevaporated Cu(In, Ga)Se<sub>2</sub> thin films in highly efficient solar cell devices, *Thin Solid Films* 515 (2007) 6217.
- [5] H. Mönig, C.-H. Fischer, R. Caballero, C.A. Kaufmann, N. Allsop, M. Gorgoi, et al., Surface Cu depletion of Cu(In, Ga)Se<sub>2</sub> films: an investigation by hard X-ray photoelectron spectroscopy, *Acta Mater.* 57 (2009) 3645.
- [6] C.A. Kaufmann, A. Neisser, R. Klenk, R. Scheer, Transfer of Cu(In, Ga)Se<sub>2</sub> thin film solar cells to flexible substrates using an in situ process control, *Thin Solid Films* 480–481 (2005) 515.
- [7] D. Briggs, M.P. Seah, *Practical Surface Analysis*, vol. 1, John Wiley and Sons, 1990.
- [8] S. Tanuma, C.J. Powell, Calculations of electron inelastic mean free paths, 21 (2000) 165.
- [9] S. Tougaard, QUASES-IMFP-TPP2M, Version 2.2, <http://www.quases.com>.
- [10] M.B. Trzhaskovskaya, V.I. Nefedov, V.G. Yarzhevsky, Photoelectron angular distribution parameters for elements Z = 1 to Z = 54 in the photoelectron energy range 100–5000 eV, *At. Data Nucl. Data Tables* 77 (2001) 97.
- [11] M.B. Trzhaskovskaya, V.I. Nefedov, V.G. Yarzhevsky, Photoelectron angular distribution parameters for elements Z = 55 to Z = 100 in the photoelectron energy range 100–5000 eV, *At. Data Nucl. Data Tables* 82 (2002) 257.
- [12] J. Kiss, T. Gruhn, G. Roma, C. Felser, Theoretical study on the diffusion mechanism of Cd in the Cu-poor phase of CuInSe<sub>2</sub> solar cell material, *J. Phys. Chem. C* 117 (2013) 25933.
- [13] J. Kiss, T. Gruhn, G. Roma, C. Felser, Theoretical study on the structure and energetics of Cd insertion and Cu depletion of CuInSe<sub>2</sub>, *J. Phys. Chem. C* 117 (2013) 10892.
- [14] T. Nakada, A. Kunioka, Direct evidence of Cd diffusion into Cu(In, Ga)Se<sub>2</sub> thin films during chemical-bath deposition process of CdS films, *Appl. Phys. Lett.* 74 (1999) 2444.
- [15] S. Sadewasser, W. Bremsteller, T. Plake, C.A. Kaufmann, C. Pettenkofer, Microscopic investigation of the CdS buffer layer growth on Cu(In, Ga)Se<sub>2</sub> absorbers, *J. Vac. Sci. Technol. B Microelectron. Nanom. Struct.* 26 (2008) 901.